Abstract

Background The anti-epileptic drug vigabatrin is associated with visual field loss (VAVFL) and thinning of the peripapillary retinal nerve fibre layer (PPRNFL), thereby implicating retinal ganglion cell (RGC) dysfunction.

Objective The objective of the study was to determine the relationship between the two outcomes in order to improve the risk/ benefit analysis of vigabatrin, particularly in those unable to undertake perimetry.

Methods A retrospective cross-sectional observational design identified 40 adults who had received vigabatrin for refractory seizures and who had undergone a combined protocol of perimetry and optical coherence tomography (OCT) of the PPRNFL. Two established models successfully applied to other optic neuropathies were used to evaluate, topographically, the function-structure relationship for the superior and inferior retinal quadrants.

Results The function-structure relationship for each model was consistent with other optic neuropathies. With the first model, PPRNFL thinning, expressed in μm, asymptoted at an equivalent visual field loss of worse than approximately -10.0dB, thereby preventing assessment of more substantial thinning. The second model overcame the asymptote by transforming the outcomes to RGC soma and axon estimates, respectively; the latter were linearly related.

Conclusions Concurrent use of perimetry and OCT, enabling reciprocal validation, is essential for the detection and assessment of vigabatrin toxicity. However, OCT affords a limited measurement range compared to perimetry: severity cannot be directly assessed when the PPRNFL quadrant thickness is less than approximately 65μm, depending upon the type of tomographer. This limitation can be overcome by transformation of thickness to remaining axons, an outcome requiring input from perimetry.

1.0 Introduction

Vigabatrin was introduced outside of the USA in 1989 as add-on therapy for adults with refractory focal seizures and as monotherapy for infantile spasms [1-2]. It gained FDA approval for these uses in 2009. The pattern of vigabatrin usage in the USA over the five year period ending 2014 has been documented for adults [3] and for infants [4].

Vigabatrin is associated with irreversible visual field loss (VAVFL) [5-10]. The frequency of VAVFL in adults, modelled from cross-sectional evidence, increases rapidly in the first two years (2kg cumulative dose) of treatment [11-12] and plateaus at 75-80% after approximately six years duration (5kg cumulative dose) [12]. The field loss manifests as a bilateral, and clinically symmetrical, 'concentric' constriction. When present within the central field, the field loss, by probability analysis of standard automated perimetry (SAP), exhibits a steep sided bi-nasal annulus which extends, to varying amounts, vertically across the horizontal midline and also centripetally. In severe manifestations, the field loss is concentric to within approximately 15º from fixation [8].

Vigabatrin is also associated with a thinning of the peripapillary retinal nerve fibre layer (PPRNFL) [13-18]. The assessment of the PPRNFL by optical coherence tomography (OCT), a rapid, objective and non-invasive imaging technique, yields a characteristic bilateral and clinically symmetrical pattern of damage in adults [15-17] and children [18]: namely, superior and/ or inferior quadrant thinning, with or without nasal quadrant thinning, and a normal temporal quadrant thickness. The temporal quadrant exhibits thinning only in cases of concentric field loss within the central field [15]. However, one study has reported that the PPRNFL thickness increases with initial exposure to vigabatrin [19] whilst another suggests

that PPRNFL thinning in adults is associated with epilepsy and with anti-epileptic drug resistance, in particular [20].

The characteristics of the VAVFL and of the concomitant PPRNFL thinning are compatible with a subtle nasal [21] or 'inverse' [22] optic atrophy, i.e., that sparing the temporal sector of the optic nerve head which contains the axons from the papillomacular bundle. They are also compatible with the retinal histology at post mortem of an individual with VAVFL [23]. However, VAVFL is also associated with a reduction in the amplitude of the 30Hz flicker cone electroretinogram response, thereby implicating the cone pathway [24-25].

The function-structure association between the severity of the VAVFL and the extent of the PPRNFL thickness has received little attention [14, 16-17]. However, any association is potentially confounded by the non-axonal component of OCT reflectance in advanced disease, i.e., that arising from glial cells etc., which prevents measurement of the PPRNFL below approximately 45μm [26] depending upon the type of tomographer. In addition, any topographical variation in the association has not been evaluated.

The lack of clarity in the relationship between the functional and structural abnormalities in vigabatrin toxicity is clinically concerning given the requirement to maintain the balance between the optimum treatment of the epilepsy and the prevention of irreversible visual dysfunction. Such concern is paramount in the management of infantile spasms, where perimetry is not viable until at least a developmental age of eight years [24], and in at least 20-25% of adults exposed to vigabatrin who are unable to undertake a visual field examination reliably [17, 24].

Although various models have been proposed [27], two distinctly different models have gained popularity for the description of the function-structure association in diseases involving the retinal ganglion cells [28-29]. The model of Hood [28], which is confounded by the non-axonal component of OCT reflectance, yields an exponential function in primary open-angle glaucoma [30], ischaemic optic neuropathy [31] and optic neuritis [32] between the PPRNFL thickness, by quadrant, and the mean of the corresponding age-corrected central visual field loss. The empirically derived model of Harwerth and colleagues [29] compensates for the non-axonal component of OCT reflectance. It yields a strong linear association in primary open-angle glaucoma [29] between the estimated number of remaining retinal ganglion cell soma at each stimulus location, calculated from the central field outcome, and the estimated number of remaining ganglion cell axons, based upon the PPRNFL thickness derived by OCT, at the topographically corresponding position of entry into the optic nerve head. Given the involvement, either as a primary or as a secondary outcome, of the PPRNFL and, thus, the retinal ganglion cells in the pathogenesis of vigabatrin toxicity, it can be hypothesized that both models would exhibit a strong topographical function-structure relationship. Such an outcome, if present, would inform the detection, and assessment of any progression, of the toxicity.

The primary purpose of the study, therefore, was to determine the function-structure relationship in vigabatrin toxicity using the models of Hood [28] and Harwerth [29]. The secondary aim was to determine the associations between the estimated numbers of remaining ganglion cell soma and axons, derived from the Harwerth model, and the extent of exposure to vigabatrin. Such outcomes would enable refinement of the continuous risk/ benefit assessment necessary for patients receiving vigabatrin.

2.0 Methods

The study utilized a retrospective cross-sectional observational design.

2.1 Cohort

A case series of 40 individuals, who had previously been treated with vigabatrin as add-on therapy for refractory seizures, was identified from those attending the Alan Richens Unit of the Welsh Epilepsy Centre, University Hospital of Wales, Cardiff, UK. Of these, 30 had focal seizures, six generalized and four of unknown onset. All individuals had undergone ophthalmological examination and conformed to standard inclusion criteria adopted for studies involving perimetry [33], particularly in regard to an absence of visual pathway abnormality identified by whole-brain magnetic resonance imaging (MRI) [16] and the ensuing retrograde trans-synaptic degeneration of the PPRNFL [34]. They had all completed a reliable outcome on at least two occasions to a standardized protocol of perimetry and OCT.

A second cohort of 11 consecutively presenting normal individuals, who had taken part in a separate study which had utilized a similar methodology, was used as a control. They were recruited from those attending the Cardiff University Eye Clinic and all conformed to inclusion criteria identical to that of the cohort exposed to vigabatrin with the exception that none were epileptic and none had undergone whole-brain MRI. The cohort was older than that exposed to vigabatrin.

2.2 Perimetry

The visual field examinations conformed to the protocol approved by the European Medicines Agency for the detection of VAVFL: in this instance, Three Zone age-corrected suprathreshold perimetry of the central and peripheral field using the Full Field 135 Point Screening Test and

SAP of the central field using the Central 30-2 Threshold Test and the FASTPAC strategy of the Humphrey Field Analyzer 750 (Carl Zeiss, Meditec, Dublin, CA) [35].

The normal individuals had all undergone SAP in each eye using the Central 24-2 Threshold Test and the SITA Standard strategy of the Humphrey Field Analyzer 750. All had previously undertaken perimetry as part of their routine clinical care.

Inclusion criteria for the reliability of the outcome of the visual field examination comprised ≤15% incorrect responses to the false-positive catch trials; ≤20% incorrect responses to the fixation loss catch trials and/ or good quality outcomes to the gaze tracking; and ≤30% incorrect responses to the false-negative catch trials, the tolerance widened with increase in severity of the field loss [36].

The visual fields were selected from the most recent visit at which the reliability criteria had been met. They were reviewed at the end of the inclusion phase, masked to the given cohort, in random order by one of the authors (JMW) who is highly experienced in interpreting the visual fields from patients exposed to vigabatrin [8-9, 35]. The outcome was classified on the appearance of, and the consistency between, the peripheral and the central fields.

2.3 Optical Coherence Tomography

Measurement of the PPRNFL thickness had been undertaken using the standard 3.4 Scan protocol of the StratusOCT (Carl Zeiss, Meditec, Dublin, CA). The pupils were dilated, if necessary, with one drop of 0.5% tropicamide and one drop of 2.5% phenylephrine hydrochloride. The polarization and Z-axis offset were optimized to gain maximum reflection

of the signal. Between three and seven images were retained for each individual. All retained images were free from blink or movement artefacts and had a signal to noise ratio of ≥ 33dB.

The OCT images from the visit corresponding to that selected for the visual field outcome were reviewed in random order by two authors (SA and CK), independently of one another. Both authors were masked to the cohort and to the outcome of the perimetry. The images which possessed the optimal placement of the scan centre, compatible with the maximum signal to noise ratio, were selected for each individual. The PPRNL thickness was calculated as the mean of the thicknesses from the retained images.

2.4 Modelling

2.4.1 Hood model

The Hood model was separately constructed for the superior and the inferior quadrants (Online Supporting Information; Appendix 1). Briefly, the quadrant PPRNFL thickness and the mean of the Total Deviation values (defined as the measured differential light sensitivity at the given location minus the age-corrected normal value) across the stimulus locations within the corresponding quadrant of the central field were obtained for each individual. The ensuing association was described by the exponential function which is defined by two parameters: the quadrant mean Total Deviation of each normal individual and the quadrant PPRNFL thicknesses of those individuals exposed to vigabatrin with a Total Deviation of worse than -10dB.

2.4.2 Harworth model

The Harworth model was separately constructed for the superior and the inferior quadrants (Online Supporting Information; Appendix 2). Briefly, the number of remaining ganglion cell

soma at each stimulus location within the central field was calculated from the differential light sensitivity and summed to give the total number for the given quadrant. The number of remaining ganglion cell axons at each corresponding stimulus location was calculated from the PPRNFL thickness and summed to give the quadrant total. The topographical relationship between each stimulus location and the corresponding position of the axonal entry at the optic nerve head followed that of an established model [37].

The visual field and PPRNFL outcomes of the normal individuals, applied to each model, were separately adjusted to the age of the individuals exposed to vigabatrin based upon the respective slopes of the relationships with age [38-39].

2.5 Analysis

The characteristics of those with and without VAVFL were described with summary statistics. Differences in a given summary statistic were evaluated, as appropriate, using Analysis of Variance and/ or Co-variance and/ or independent t-tests for continuously distributed variables and Chi-square or Fishers Exact tests for categorical variables.

The structure-function relationships for the two models were illustrated by separate scatter plots. For the Hood model, the confidence intervals associated with the asymptote were calculated from the medians of 100,000 samples generated by statistical bootstrapping. For the Harwerth model, any differences between the three groups in the relationship between the remaining ganglion cell soma and the remaining axons were investigated using Principal Component Analysis. Briefly, two successive linear transformations were undertaken of the relationship. The first translation was undertaken such that the origin coincided with the means of the values along the x- and along the y-axes. The second translation involved rotation of the

axes such that the x-axis coincided with the line of best linear fit through the data. The first principal component enabled an estimate of the total number of retinal ganglion cells based upon the soma and axon estimates. The second principal component described the similarity between the three groups in the relationship between the estimates of the soma and axon quantities. This latter component increased with increase in the disparity between the two estimates; a higher number indicated a greater estimate of soma. The differences in the distribution of each component between the three groups were evaluated using the Mann-Whitney Test.

The correlations between the estimated number of remaining ganglion cell soma and axons and the duration and cumulative dose of vigabatrin were determined by Pearson Product Moment Correlation.

The datasets generated during and/ or analysed during the current study are available from the corresponding author on reasonable request.

3.0 Results

3.1 Cohort demography

The demographic characteristics of the cohort exposed to vigabatrin are shown in Table 1. The cohort contained more females than males (χ^2 = 6.4; p=0.026). The males were slightly older than the females at the time of perimetry and OCT but this difference did not reach statistical significance (difference between means 4.26 years 95% CI -4.65 to 11.18; p=0.840). Twenty-four of the 40 individuals exhibited VAVFL. All but one of these 24 individuals exhibited visual field loss within the central field. The difference in the proportion with VAVFL by gender, 11 out of 15 males and 13 out of 25 females, was not statistically significant (p=0.188). The age of the individuals with VAVFL at the time of perimetry and OCT was identical to those exposed to vigabatrin but with normal fields (difference between means -0.24 years, 95% CI -7.77 to 7.30; p=0.952). The duration and cumulative dose of vigabatrin therapy were highly correlated (r=0.849, p<0.001). Those with VAVFL manifested a greater exposure to vigabatrin (difference between means 6.27kg, 95% CI 3.11 to 9.40, p<0.003; and 4.95 years, 95% CI 2.02 to 7.88; p<0.001) and a shorter time from withdrawal (difference between means -4.1 years, 95% CI -6.49 to -1.71; p<0.001).

The functional and structural characteristics of the cohort exposed to vigabatrin, averaged across the two eyes, are shown in Table 2. The two most common summary measures for describing the severity of central visual field loss, the Mean Deviation and the Pattern Standard Deviation, were each similar between the right and left eyes (p=0.34) and were worse in each eye (p<0.001) for the individuals with VAVFL than for those without the toxicity. The difference between the means of those with and without VAVFL for the two eyes, combined, was -7.59dB (95% CI -8.96 to -1.37; p<0.001) and 5.91dB (95% CI 4.90 to 7.33 p<0.001) respectively.

The thickness of the PPRNFL was similar between the right and left eyes (p=0.08), varied between quadrants (p<0.001) and was thinner in each eye for the individuals with VAVFL than for those without the toxicity and was thickest for the normal individuals (p<0.001). The overall PPRNFL, for the two eyes combined, was substantially thinner for those with VAVFL than for those without (difference between means -86.4µm, 95% CI -110.0 to -62.8; p<0.001). The overall PPRNFL for those without the toxicity was thinner than that for the normal individuals even though the latter exhibited additional thinning due to the older age: for the overall thickness of the two eyes combined, the difference in the means was -37.3µm (95% CI -65.2 to 9.4; p<0.001).

3.2 Hood Model

The relationship between the PPRNFL thickness and the mean Total Deviation, relative to the exponential function (solid line), for the superior and inferior quadrants for each individual in each of the three groups is given in Figure 1 for the right and left eyes, separately. The asymptotes, and the corresponding 95% confidence intervals, for the superior and inferior quadrants of the right eye were 59.9µm (53.0 to 78.3) and 62.4µm (47.0 to 82.0), respectively, and for the left eye 67.4µm (50.0 to 85.3) and 68.8µm (60.5 to 75.8).

3.3 Harworth Model

The relationship between the remaining ganglion cell soma and the remaining ganglion cell axons for the superior and inferior meridians for each individual in each of the three groups is given in Figure 2 for the right and left eyes, separately. The estimated number of remaining ganglion cell soma was greater than that for the remaining ganglion cell axons.

The outcome of the principal components analysis of the relationship given in Figure 2 is shown in Figure 3. Those with VAVFL exhibited fewer remaining ganglion cells derived from the corresponding combined estimates of the soma and axons (i.e., a lower value along the First Principal Component) in each of the two quadrants for each eye, compared to those exposed to vigabatrin but with normal fields (all $p \leq 0.001$) and also compared to the normal individuals (all $p \leq 0.001$). Those exposed to vigabatrin with normal fields had fewer ganglion cells than the normal individuals ($p \leq 0.001$ to $p < 0.05$). There was no difference between the three groups in the relationships between the two estimates of the ganglion cell characteristics (i.e., along the Second Principal Component).

3.4 Correlation with vigabatrin exposure

The Coefficients of Determination between the estimates of the remaining soma and axons for the superior and inferior quadrants and the cumulative dose and duration of vigabatrin therapy, at the time of detection of the field loss, are given in Table 4. Almost all the Coefficients were higher for cumulative dose than for duration and were highest (approximately 42%) both for the Total Deviation and for the estimated number of remaining axons.

4.0 Discussion

This study provides the first quantitative confirmation of the topographical correspondence between the central visual field and the PPRNFL outcomes in vigabatrin toxicity. Both models yielded strong function-structure relationships, similar to those for other optic neuropathies [29-32], and validated each model to the other. Such outcomes indicate that, in individuals with vigabatrin toxicity, perimetry and OCT of the PPRNFL implicate the same underlying dysfunction, i.e., retinal ganglion cell abnormality.

The fundamental strength of the study lies in the extensive range of exposure to vigabatrin (0.33 to 16.1 years) and of severity of VAVFL (MD -1.62 to -22.81; PSD 2.65 to 13.04); such ranges provide an unequivocal insight into the effect of the toxicity over the longer term.

The outcome from the Hood model demonstrates the impact of the non-axonal component of OCT reflectance on the management of vigabatrin toxicity. An assessment of the severity of the PPRNFL thickness, when expressed in μm, was only possible where the equivalent visual field loss was within a mean Total Deviation of approximately -10.0dB after which the value of the PPRNFL thickness reached an asymptote. In the current study, 9 of the 24 individuals with VAVFL exhibited mean Total Deviations of worse than -10.0dB in both quadrants of each eye.

The Harwerth model empirically overcomes the non-axonal component of reflectance by the use of a correction factor, based upon the mean Total Deviation. It expresses the PPRNFL thickness as a continuous scale in terms of the number of remaining axons and enables an assessment of the full range of PPRNFL thinning associated with vigabatrin toxicity. The

overestimation of the number of remaining ganglion cell soma in each quadrant compared to the number of remaining axons was similar to that for primary open-angle glaucoma [29] and is a limitation of the model [40].

The definition of vigabatrin retinal toxicity was based upon the outcome of perimetry rather than of OCT. All 24 individuals exhibited the characteristic pattern of PPRNFL thinning associated with vigabatrin toxicity [13-18]. Of these, two exhibited temporal quadrant thinning in association with severe VAVFL.

Of the 16 individuals without VAVFL, 8 exhibited a normal PPRNFL thickness in each eye for each of the four quadrants relative to the age-corrected normal values proprietary to the manufacturer. Three individuals exhibited bilateral and symmetrical abnormal PPRNFL thinning in either the superior or inferior quadrants, only, which lay at the fifth or lower percentiles of the proprietary normal values. Such a pattern of thinning is associated with vigabatrin toxicity [13-18] and may have been an earlier marker than the field loss. The remaining five individuals each exhibited abnormal thinning (between the fifth and first percentiles) in one randomly distributed quadrant of one eye. Such an outcome was not associated with visual field loss and was most likely to have arisen from the difficulty in achieving quality fixation during the scan acquisition. This is a common problem in individuals with severe epilepsy. Nevertheless, as a group, the PPRNFL thicknesses were statistically significantly thinner than those for the normal individuals. Such a finding is in accord with the outcome reported in drug resistant epilepsy [20].

All 11 individuals exhibited normal visual fields and normal PPRNFL thicknesses, defined in terms of probability/ percentile analyses relative to the distributions of the age-corrected

normal values proprietary to each type of instrument, thereby confirming the validity of the authors' review procedure.

The Coefficient of Determinations between the cumulative dose and duration of vigabatrin and the various estimates of function and structure were modest and are compatible with the concept of an idiopathic drug reaction [16-17]; however, it was clear that functional and structural damage unquestionably worsened with increase in exposure to vigabatrin. This latter finding is compatible with cross-sectional evidence that the risk of developing vigabatrin toxicity increases with increasing exposure to vigabatrin [11-12]. Such relationships further underline the importance of regular assessments of individuals undergoing therapy with vigabatrin.

Both models are based upon the presence of VAVFL manifesting within the central field. However, it should be remembered that VAVFL is a peripheral defect which subsequently encroaches, to varying extents, into the central field. Both models are also dependent upon the overall differential light sensitivity, i.e. that arising from both the optical quality and the integrity of the neural processing. The attenuation due to optical degradation was minimized by excluding those manifesting a cataract, or other disturbances of the ocular media, from the case series and by ensuring that the appropriate refractive correction was used for the viewing distance of the perimeter. Optical degradation worsens the Total Deviation outcome utilized in the Hood model and erroneously decreases, by similar magnitudes, the estimated numbers of ganglion cell soma and axons in the Harwerth model. However, toxicity encroaching into the central field can still be identified by perimetry in the presence of optical degradation since the diagnosis is based upon the characteristic shape of the field loss manifested by Pattern Deviation probability analysis.

Both models were developed from the outcomes of the visual field examination with the Humphrey Field Analyzer and of OCT with the StratusOCT; both of these instruments were used in the current study. The models have subsequently been successfully applied, in primary open-angle glaucoma, to the outcome from spectral domain OCT [40] which has superseded time domain OCT. Compared to time domain OCT, spectral domain OCT exhibits improved axial and lateral resolution, by approximately 5μm, and a faster B scan acquisition time; but a relative reduction in detector performance. In addition, most spectral domain systems also incorporate software to compensate for poorly aligned images. However, the operator variability is similar [41] and the PPRNFL thickness by each technique gives similar sensitivities and specificities for the detection of early to moderate primary open-angle glaucoma [42-43] and for multiple sclerosis [44], retrobulbar optic neuritis and non-arteritic ischemic optic neuropathy [45]. The use of spectral domain OCT in the current study would merely have resulted in slight instrument-dependent differences in the absolute thickness of the PPRNFL [41, 45]. Such differences would not have materially affected the strong relationship between function and structure in vigabatrin toxicity which has been demonstrated in the current study.

5.0 Conclusion

Perimetry enables an assessment of the severity of vigabatrin toxicity regardless of the extent of PPRNFL thinning. When OCT is used as the primary investigative modality and thinning is suspected, a concurrent peripheral and central visual field examination should be undertaken, whenever possible, to confirm the presence of VAVFL. The severity of vigabatrin toxicity can only be directly assessed by OCT when the superior and/ or inferior quadrant PPRNFL thicknesses are greater than approximately 65μm, depending upon the type of tomographer. Below this value (equivalent to a quadrant Total Deviation within the central field of worse

than approximately -10.0dB) severity can only be evaluated in terms of the number of remaining axons, an outcome dependent on perimetry.

Compliance with Ethical Standards

Funding SA was supported by an unrestricted grant from the Ministry of Higher Education, Kingdom of Saudi Arabia. The latter had no role in the design and conduct of the study; collection, management, analysis, and interpretation of the data; or preparation of the manuscript.

Conflict of Interest JMW, SA, PEMS and CK declare that they have no conflict of interest.

Ethical approval All procedures performed in studies involving human participants were in accordance with ethical standards of the Local Research and Ethics Committee and with 1964 Helsinki declaration and its later amendments or comparable ethical standardsand the study had approval from the Local Research and Ethics Committee. For this type of study, formal consent is not required.

REFERENCES

1. Mumford JP, Dam M. Meta-analysis of European placebo controlled studies of vigabatrin in drug resistant epilepsy. Br J Clin Pharmacol. 1989;27(Suppl 1):S101-7.

2. Appleton RE, Peters AC, Mumford JP, Shaw DE. Randomised, placebo controlled study of vigabatrin as first-line treatment of infantile spasms. Epilepsia 1999;40(11):1627-33.

3. Krauss G, Faught E, Foroozan R, Pellock JM, Sergott RC, Shields WD, et al. Sabril® registry 5-year results: Characteristics of adult patients treated with vigabatrin. Epilepsy Behav. 2016;56(3):15-19.

4. Pellock JM, Faught E, Foroozan R, Sergott RC, Shields WD, Ziemann A, et al. Which children receive vigabatrin? Characteristics of pediatric patients enrolled in the mandatory FDA registry. Epilepsy Behav. 2016;60(7):174-180.

5. Eke T, Talbot JF, Lawden MC. Severe persistent visual field constriction associated with vigabatrin. BMJ. 1997;314(7075):180-1.

6 Miller NR, Johnson MA, Paul SR, Girkin CA, Perry JD, Endres M, et al. Visual dysfunction in patients receiving vigabatrin: clinical and electrophysiologic findings. Neurology 1999;53(9):2082-87.

7. Kälviäinen R, Nousiainen I, Mäntyjärvi M, Nikoskelainen E, Partanen J, Partanen K, et al. Vigabatrin, a gabaergic antiepileptic drug, causes concentric visual field defects. Neurology 1999;53(5):922-26.

8. Wild JM, Martinez C, Reinshagen G, Harding GF. Characteristics of a unique visual field defect attributed to vigabatrin. Epilepsia 1999;40(12):1784-94.

9. Lawden MC, Eke T, Degg C, Harding GF, Wild JM. Visual field defects associated with vigabatrin therapy. J Neurol Neurosurg Psychiatry. 1999;67(6):716-22.

10. Daneshvar H, Racette L, Coupland SG, Kertes PJ, Guberman A, Zackon D. Symptomatic and asymptomatic visual loss in patients taking vigabatrin. Ophthalmology1999;106(9):1792-98.

11. European Medicines Agency. Opinion of the Committee for proprietary medicinal products pursuant to Article 12 of Council Directive 75/319/EEC as amended for vigabatrin. Annex 1. Scientific conclusions and grounds for amendment of the summaries of product characteristics presented by the EMEA. 1999, European Medicines Agency, Canary Wharf, London, United Kingdom. Available at: http://www.ema.europa.eu/docs/en_GB/document_library/Referrals_document/Vigabatrin_31/WC500014088.pdf Accessed 25th February 2018.

12. Wild JM, Fone DL, Aljarudi S, Lawthom C, Smith PE, Newcombe RG, et al. Modelling the risk of visual field loss arising from long-term exposure to the antiepileptic drug vigabatrin: A cross-sectional approach. CNS Drugs 2013;27(10):841-9.

13 Choi HJ, Kim DM. Visual field constriction associated with vigabatrin: retinal nerve fiber photographic correlation. J Neurol Neurosurg Psychiatry. 2004;75(10):1395.

14. Wild JM, Robson CR, Jones AL, Cunliffe IA, Smith PE. Detecting vigabatrin toxicity by imaging of the retinal nerve fiber layer. Invest Ophthalmol Vis Sci. 2006;47(3):917-24.

15. Lawthom C, Smith PEM, Wild JM. Nasal retinal nerve fiber layer attenuation: a biomarker for vigabatrin toxicity. Ophthalmology 2009;116(3):565-571.

16. Clayton LM, Devile M, Punte T, Kallis C, de Haan GJ, Sander JW, et al. Retinal nerve fiber layer thickness in vigabatrin-exposed patients. Ann Neurol. 2011;69(5):845-54.

17. Clayton LM, Devile M Punte T de Haan GJ, Sander JW, Acheson JF et al. Patterns of peripapillary retinal nerve fiber layer thinning in vigabatrin-exposed individuals. Ophthalmology 2012;119(10):2152-60.

18. Origlieri C, Geddie B, Karwoski B, Berl MM, Elling N, McClintock W, et al. Optical coherence tomography to monitor vigabatrin toxicity in children. J AAPOS. 2016;20(2):136-40.

19. Sergott RC, Johnson CA, Laxer KD, Wechsler RT, Cherny K, Whittle J, et al. Retinal structure and function in vigabatrin-treated adult patients with refractory complex partial seizures. Epilepsia 2016;57(10):1634-42.

20. Balestrini S, Clayton LM, Bartmann AP, Chinthapalli K, Novy J, Coppola A, et al. Retinal nerve fiber layer thinning is associated with drug resistance in epilepsy. J Neurol Neurosurg Psychiatry. 2016:87(4);396-401.

21. Frisen L, Malmgren K. Characterization of vigabatrin associated optic atrophy. Acta Ophthalmol Scand. 2003;81(5):466-73.

22. Buncic JR, Westall CA, Panton CM, Munn JR, MacKeen LD, Logan WJ. Characteristic retinal atrophy with secondary "inverse" optic atrophy identifies vigabatrin toxicity in children. Ophthalmology 2004;111(10):1935-42.

23. Ravindran J, Blumbergs P, Crompton J, Pietris G, Waddy H. Visual field loss associated with vigabatrin: pathological correlations. J Neurol Neurosurg Psychiatry. 2001;70(6):787-9.

24. Harding GF, Wild JM, Robertson KA, Rietbrock S, Martinez C. Separating the retinal electrophysiologic effects of vigabatrin. Treatment versus field loss. Neurology 2000;55(3):347-52.

25. Wright T, Kumarappah A, Stavropoulos A Reginald A, Buncic JR, Westall CA. Vigabtrin toxicity in infants is associated with retinal defect in adolescence. A prospective observational study. Retina 2017;37(5):858-66.

26. Sihota R, Sony P, Gupta V, Dada T, Singh R. Diagnostic capability of optical coherence tomography in evaluating the degree of glaucomatous retinal nerve fiber damage. Invest Ophthalmol Vis Sci. 2006;47(5):2006-10.

27. Price, DA, Swanson WH, Horner DG. Using perimetric data to estimate ganglion cell loss for detecting progression of glaucoma: a comparison of models. Ophthalmic Physiol Opt. 2017;37(4):409-19.

28. Hood DC. Relating nerve fiber layer thickness to behavioural sensitivity in patients with glaucoma. The application of a linear mode. J Opt Soc Am. 2007;24(5):1426-30.

29. Wheat JL, Rangaswamy NV, Harwerth RS. Correlating RNFL thickness by OCT with perimetric sensitivity in glaucoma patients. J Glaucoma 2012;21(2):95-101.

30. Hood DC, Anderson S, Wall M, Kardon RH. Structure versus function in glaucoma: an application of a linear model. Invest Ophthalmol Vis Sci. 2007;48(9):3662-8.

31. Hood DC, Anderson S, Rouleau J, Wenick AS, Grover LK, Behrens MM, et al. Retinal nerve fiber layer structure versus visual field function in patients with ischemic optic neuropathy. A test of a linear model. Ophthalmology 2008;115(5):904-10.

32. Cheng H, Laron M, Schiffman JS, Tang RA, Frishman LJ. The relationship between visual field and retinal nerve fiber layer measurements in patients with multiple sclerosis. Invest Ophthalmol Vis Sci. 2007;48(12):5798-805.

33. Vonthein R, Rauscher S, Paetzold J, Nowomiejska K, Krapp E, Hermann A, et al. The normal age-corrected and reaction time-corrected isopter derived by semi-automated kinetic perimetry. Ophthalmology 2007;114(6):1065-72.

34. Jindahra P, Petrie A, Plant GT. The time course of retrograde trans-synaptic degeneration following occipital lobe damage in humans. Brain 2012;135(2):534-41.

35. Wild JM, Chiron C, Ahn H, Baulac M, Bursztyn J, Gandolfo E, et al. Visual field loss in patients with refractory partial epilepsy treated with vigabatrin: final results from an open-label, observational, multicenter study. CNS Drugs 2009;23(11):965-82.

36. Bengtsson B, Heijl A. False-negative responses in glaucoma perimetry: indicators of patient performance or test reliability? Invest Ophthalmol Vis Sci. 2000;41(8):2201-04.

37. Garway-Heath DF, Poinoosawmy D, Fitzke FW, Hitchings RA. Mapping the visual field to the optic disc in normal tension glaucoma eyes. Ophthalmology 2000;107(10):1809-15.

38. Heijl A, Lindgren G, Olsson J. Normal variability of static perimetric threshold values across the central visual field. Arch Ophthalmol. 1987;105(11):1544-49.

39. Parikh RS, Parikh SR, Sekhar GC, Prabakaran S, Babu JG, Thomas R. Normal age-related decay of retinal nerve fiber layer thickness. Ophthalmology 2007;114(5):921-26.

40. Raza AS, Hood DC. Evaluation of a method for estimating retinal ganglion cell counts using visual fields and optical coherence tomography. Invest Ophthalmol Vis Sci. 2015; 56(9):2254-68.

41. Pierro L, Gagliardi M, Iuliani L, Ambrosi A, Bandello F. Retinal nerve fiber layer thickness reproducibility using seven different OCT combinations. Invest Ophthalmol Vis Sci. 2012; 53(9):5912-20.

42. Chang RT, Knight OJ, Feuer WJ, Budenz DL. Sensitivity and specificity of time-domain versus spectral-domain optical coherence tomography in diagnosing early to moderate glaucoma. Ophthalmology 2009:116(12):2294-99.

43. Jeoung JW, Park KH. Comparison of the Cirrus OCT and Stratus OCT on the ability to detect localized retinal nerve fiber layer defects in pre-perimetric glaucoma. Invest Ophthalmol Vis Sci. 2010; 51(2):938-45.

44. Watson GM, Keltner JL, Chin EK, Harvey D, Nguyen A, Park SS. Comparison of retinal nerve fiber layer and central macular thickness measurements among five different optical coherence tomography instruments in patients with multiple sclerosis and optic neuritis. J Neuroophthalmol. 2011;31(2):110-6.

45. Giambene B, Virgili G, Menchini U. Retinal nerve fiber layer thickness by Stratus and Cirrus OCT in retrobulbar optic neuritis and nonarteritic ischemic optic neuropathy. Eur J Ophthalmol. 2017;27(1):80-5.

		EXPOSED TO VIGABATRIN		NORMAL INDIVIDUALS
		VAVFL	Normal	
Gender	Male	11	4	6
	Female	13	12	5
Age (Yrs)	Mean	43.6	43.8	72.1
	SD	12.9	10.5	15.1
	Median	44.3	45.5	72.1
	IQR	32.3, 52.0	38.9, 50.0	59.8, 77.8
	Range	22.8 to 68.6	19.0 to 60.2	30.9 to 81.5
Cumulative dose of vigabatrin (kg)	Mean	10.6	4.3	
	SD	5.2	4.6	
	Median	11.0	2.4	
	IQR	6.7, 14.4	5.2, 14.2	
	Range	2.5 to 19.4	0.69 to 14.2	
Duration of vigabtrin (Yrs)	Mean	10.9	5.9	
	SD	3.4	5.0	
	Median	11.7	5.1	
	IQR	9.2, 13.4	9.0, 14.5	
	Range	3.6 to 16.1	0.33 to 14.5	
Time from withdrawal of vigabatrin (Yrs)	Mean	6.6	10.7	
	SD	2.6	4.3	
	Median	6.5	8.9	
	IQR	5.4, 7.3	8.1, 13.4	
	Range	0.3 to 12.6	4.7 to 19.2	

Table 1 The summary statistics for the demographic characteristics of the 40 individuals exposed to vigabatrin by visual field outcome and for the normal individuals

VAVFL vigabatrin-associated visual field loss

		EXPOSED TO VIGABATRIN		NORMAL INDIVIDUALS
		VAVFL	**Normal Visual field**	
Mean Deviation (dB)	Mean	-8.96	-1.37	0.09
	SD	6.17	1.79	1.17
	Median	-7.58	-0.89	-0.08
	IQR	-12.06, -3.95	-2.23, -0.12	-062, 1.05
	Range	-22.81 to -1.62	-5.1 to 0.78	-1.91 to 1.85
Pattern Standard Deviation (dB)	Mean	8.21	2.30	1.53
	SD	3.37	0.49	0.33
	Median	8.22	2.16	1.47
	IQR	5.03, 11.50	1.89, 2.64	1.29, 1.72
	Range	2.65 to 13.04	1.59 to 3.7	0.96 to 2.34
PPRNFL thickness (µm)				
Superior	Mean	68.1	97.3	116.0
	SD	15.1	14.7	17.5
	Median	71.2	96.0	113.2
	IQR	57.5, 79.2	88.6, 106.4	103.0, 127.4
	Range	27.0 to 95.7	67.0 to 140.0	85.0 to 158.0
Inferior	Mean	77.3	105.8	114.3
	SD	18.4	11.1	17.1
	Median	79.9	106.2	112.0
	IQR	65.2, 88.1	101.0, 113.5	103.25. 127.4
	Range	22.9 to 128.5	81.3 to 125.3	72.0 to 137.0
Nasal	Mean	38.6	62.0	69.3
	SD	10.2	10.8	16.4
	Median	37.5	61.5	66.8
	IQR	31.9, 47.0	56.8, 70.2	56.1, 80.0
	Range	3.0 to 60.0	42.0 to 86.0	46.5 to 109.0
Temporal	Mean	64.3	68.6	72.5
	SD	12.8	10.6	12.5
	Median	64.0	61.5	74.8
	IQR	54.8, 73.0	56.8, 70.2	64.8, 78.6
	Range	39.0 to 104.0	50.0 to 89.3	49.0 to 106.0

Table 2 The summary statistics for the visual field and the PPRNFL for the 40 individuals exposed to vigabatrin by visual field outcome and for the normal individuals. Note: the Mean Deviation, the Pattern Standard Deviation and the PPRNFL thicknesses were each not significantly different between the right and left eyes and, for brevity, each outcome, is given for the two eyes, combined.
VAVFL vigabatrin-associated visual field loss, PPRNFL peripapillary retinal nerve fibre layer

		DURATION (Yrs)		CUMULATIVE DOSE (Kg)	
		Right	Left	Right	Left
Total Deviation					
	Superior	23.7	20.1	44.6	40.7
	Inferior	21.3	21.3	37.0	37.8
Number of remaining soma					
	Superior	23.7	21.0	34.9	36.1
	Inferior	12.5	19.3	24.8	26.9
PPRNFL					
	Superior	35.8	33.8	30.2	26.4
	Inferior	23.5	21.7	34.5	29.2
Number of remaining axons					
	Superior	40.5	36.5	43.8	39.7
	Inferior	29.2	27.8	37.8	36.5

Table 3 The Coefficient of Determination (R^2), expressed as a percentage, for the linear correlation between the various outcomes of perimetry and of optical coherence tomography and the duration and cumulative dose of vigabatrin

FIGURE LEGENDS

Fig 1 The outcome of the Hood model: the peripapillary retinal nerve fibre layer thickness against the mean Total Deviation for the right (left column) and left (right column) eye. The solid line indicates the exponential function. Top: superior quadrant. Bottom: inferior quadrant. The Coefficient of Determination, R^2, for each function is given in the top left of each panel

Fig. 2 The outcome of the Harwerth model: the estimated number of remaining retinal ganglion cell soma against the estimated number of remaining ganglion cell axons for the right (left column) and left (right column) eye. Top: superior quadrant. Bottom: inferior quadrant

Fig. 3 The outcome of the Principal Components analysis of the number of remaining retinal ganglion cell soma and the number of remaining ganglion cell axons for the right (left column) and left (right column) eye. Top: superior quadrant. Bottom: inferior quadrant

Figure 1

Click here to download Figure Wild_Figure 1.tif

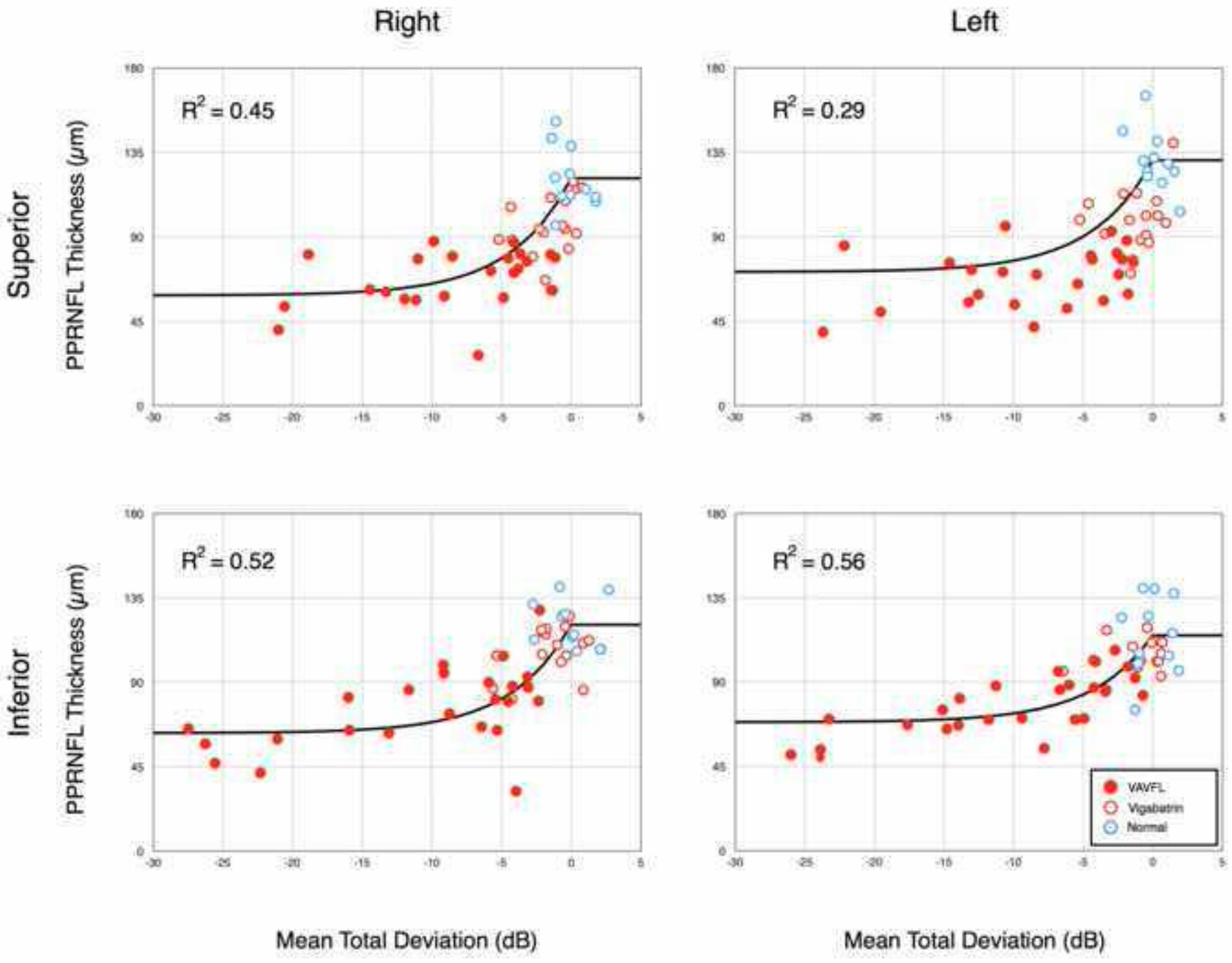

Figure 2

Click here to download Figure Wild_Figure 2.tif

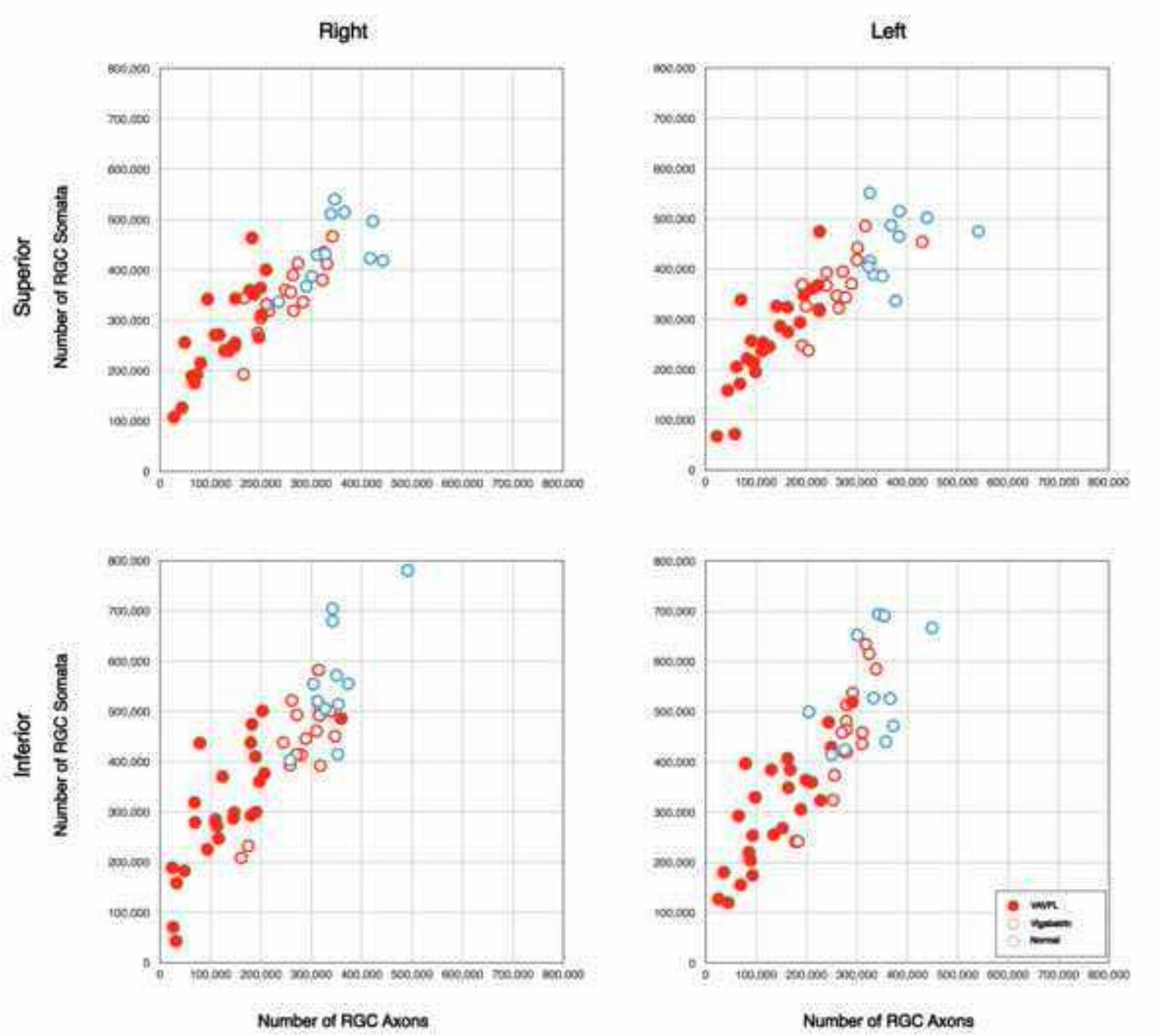

Figure 3

Click here to download Figure Wild_Figure 3.tif

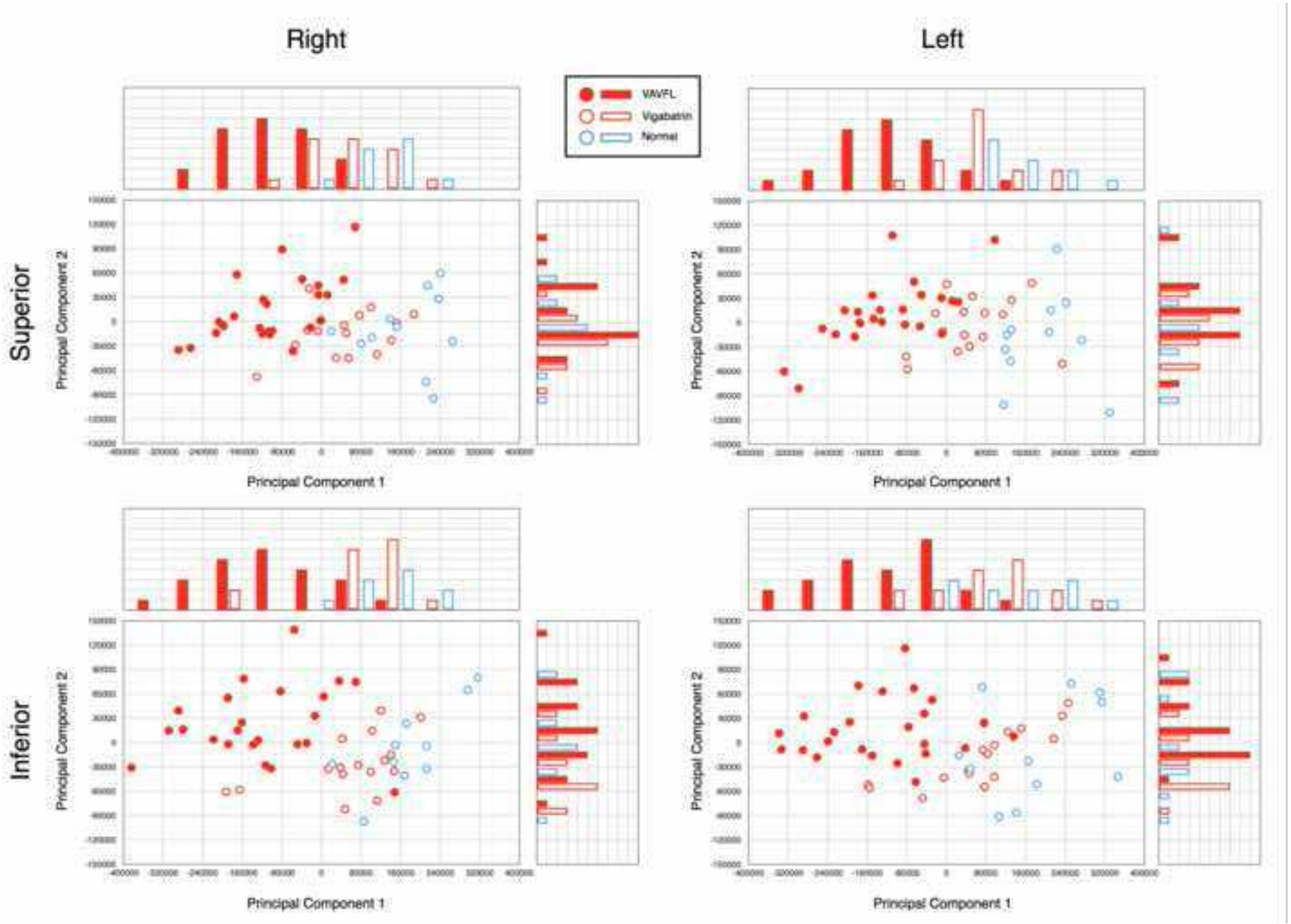

ON LINE SUPPORTING INFORMATION

1.0 APPENDIX 1

The model of Hood [1] is defined as:

$$R = s_o 10^{0.1 \times D} + b \text{ for } D \leq 0$$

and $$R = s_o + b \text{ for } D \geq 0$$

where R is the PPRNFL thickness for the given quadrant, D is the mean of the Total Deviation value for the corresponding quadrant in Program 24-2 format; s_o is the median of the PPRNFL thickness for individuals with D≤-10dB, b is the remaining thickness arising from glial tissue etc, and $s_o + b$ is the mean thickness of the normal individuals.

Reference

1. Hood DC. Relating nerve fiber layer thickness to behavioural sensitivity in patients with glaucoma. The application of a linear mode. J Opt Soc Am 2007;24(5):1426-1430.

2.0 APPENDIX 2

Ganglion cell soma quantity

The total number of retinal ganglion cell soma, $gc_{SAP,}$, across the given number of stimulus location arranged in Program 24-2 format of the Humphrey Field Analyzer, was calculated using the equations of Wheat et al [1]:

$$m = [0.054*(ecc*1.34)] + 0.9 \quad (1)$$

$$b = [-1.5*(ecc*1.34)] -14.8 \quad (2)$$

$$gl = \{[(s - 1) – b] / m\} + 4.7 \quad (3)$$

and

$$gc_{SAP} = \Sigma 10^{\wedge} (gl*0.1) \quad (4)$$

where m and b represent the slope and intercept, respectively, of the linear function of ganglion cell density (gl) by differential light sensitivity at the given eccentricity (ecc); and where gl, expressed as the number of soma per mm^2 of retina, and the differential light sensitivity (s), are each given in dB.

The constant, -1, in Equation (3) accounts for the approximate 1dB higher sensitivity of the SITA Standard algorithm compared to the Full Threshold algorithm [2-4] and was used for the calculation of the ganglion cell soma quantity for the individuals with primary open-angle glaucoma. The constant was omitted for the calculation of the ganglion cell soma quantity for the individuals exposed to vigabatrin since the differential light sensitivities obtained with the Full Threshold and FASTPAC algorithms are clinically identical [3-4]. The constant 4.7 in Equation (3) converts retinal ganglion cell soma density to the total number of retinal ganglion cell somas at the given stimulus location based upon the 6° square stimulus grid of Program 24-2.

The ganglion cell soma quantities derived by standard automated perimetry at each stimulus location were then summed, as appropriate, to give the global and each oblique quadrant total, based upon the topographical map of Garway-Heath et al 2000) [5] which relates the axons of the retinal ganglion cells sub-serving the given perimetric stimulus location to their entry point at the optic nerve head.

where m and b represent the slope and intercept, respectively, of the linear function of ganglion cell density (gl) by differential light sensitivity at the given eccentricity (ecc); and where gl, expressed as the number of soma per mm^2 of retina, and the differential light sensitivity (s), are each given in dB.

The constant, -1, in Equation (3) accounts for the approximate 1dB higher sensitivity of the SITA Standard algorithm compared to the Full Threshold algorithm [2-4] and was used for the calculation of the ganglion cell soma quantity for the individuals with primary open-angle glaucoma. The constant was omitted for the calculation of the ganglion cell soma quantity for the individuals exposed to vigabatrin since the differential light sensitivities obtained with the Full Threshold and FASTPAC algorithms are clinically identical [3-4]. The constant 4.7 in Equation (3) converts retinal ganglion cell soma density to the total number of retinal ganglion cell somas at the given stimulus location based upon the 6° square stimulus grid of Program 24-2.

The ganglion cell soma quantities derived by standard automated perimetry at each stimulus location were then summed, as appropriate, to give the global and each oblique quadrant total, based upon the topographical map of Garway-Heath et al 2000) [5] which relates the axons of the retinal ganglion cells sub-serving the given perimetric stimulus location to their entry point at the optic nerve head.

Ganglion cell axon quantity

The ganglion cell axon quantity derived by optical coherence tomography was calculated for the superior and inferior quadrants using the additional equations of Wheat et al [1] developed with the StratusOCT:

$$d = (-0.007*age) + 1.4$$

$$a = mh*px*21.1*d$$

$$c = (-0.28*mTD) + 0.18$$

and

$$ax_{oct} = 10^{\wedge}[([(\log a)*10] - c)/10]$$

where d is the axonal density, i.e. the number of axons per μm^2; age is in years, a is the number of axons for a section of the RNFL scan with a mean height (mh) in μm over px number of pixels; 21.2 is the length per pixel in μm for the 10.87 mm scan length of the standard RNFL (3.4) Scan protocol of the Stratus OCT; c is a correction factor in dB for the non-axonal component of the measured retinal nerve fibre layer thickness at the given stage of the disease, expressed by the mean of the Total Deviation values for the given visual field sector; and ax_{oct} is the age-corrected and non-axonal component-corrected total number of retinal ganglion cell axons in the given sector of the PPRNFL.

References

1. Wheat JL, Rangaswamy NV, Harwerth RS. Correlating RNFL thickness by OCT with perimetric sensitivity in glaucoma patients. J Glaucoma 2012;21(2):95-101.

ON LINE SUPPORTING INFORMATION

1.0 APPENDIX 1

The model of Hood [1] is defined as:

$$R = s_o 10^{0.1 \times D} + b \text{ for } D \leq 0$$

and $$R = s_o + b \text{ for } D \geq 0$$

where R is the PPRNFL thickness for the given quadrant, D is the mean of the Total Deviation value for the corresponding quadrant in Program 24-2 format; s_o is the median of the PPRNFL thickness for individuals with D≤-10dB, b is the remaining thickness arising from glial tissue etc, and $s_o + b$ is the mean thickness of the normal individuals.

Reference

1. Hood DC. Relating nerve fiber layer thickness to behavioural sensitivity in patients with glaucoma. The application of a linear mode. J Opt Soc Am 2007;24(5):1426-1430.

2.0 APPENDIX 2

Ganglion cell soma quantity

The total number of retinal ganglion cell soma, $gc_{SAP,}$, across the given number of stimulus location arranged in Program 24-2 format of the Humphrey Field Analyzer, was calculated using the equations of Wheat et al [1]:

$$m = [0.054*(ecc*1.34)] + 0.9 \quad (1)$$

$$b = [-1.5*(ecc*1.34)] -14.8 \quad (2)$$

$$gl = \{[(s - 1) – b] / m\} + 4.7 \quad (3)$$

and

$$gc_{SAP} = \Sigma 10^{\wedge} (gl*0.1) \quad (4)$$

2. Bengtsson B and Heijl A. Evaluation of a new perimetric threshold strategy, SITA, in patients with manifest and suspect glaucoma. Acta Ophthalmol Scand 1998;76(3):268-272.

3. Wild JM, Pacey IE, O'Neill EC, Cunliffe IA. The SITA perimetric threshold algorithms in glaucoma. Invest Ophthalmol Vis Sci 1999;40(9):1998-2009.

4. Wild JM, Pacey IE, Hancock SA, Cunliffe IA. Between-algorithm, between-individual differences in normal perimetric sensitivity: Full Threshold, FASTPAC, and SITA. Swedish Interactive Threshold algorithm. Invest Ophthalmol Vis Sci 1999;40(6):1152-1161.

5. Garway-Heath DF, Poinoosawmy D, Fitzke FW, Hitchings RA. Mapping the visual field to the optic disc in normal tension glaucoma eyes. Ophthalmology 2000;107(10):1809-1815.